THE CHEMICAL COMPOSITION OF RED GIANTS. I. DREDGE-UP IN THE M AND MS STARS

VERNE V. SMITH[1] AND DAVID L. LAMBERT[1]
Department of Astronomy, University of Texas; and McDonald Observatory
Received 1984 November 5; accepted 1985 January 16

ABSTRACT

Carbon, nitrogen, oxygen, Fe-peak, and heavy, s-process elemental abundances have been determined for nine red giants of type M and MS. The source material are high-resolution, high signal-to-noise digital spectra in the infrared and near-infrared The abundances of the Fe-peak and heavier elements are based on atomic lines and are referenced to a comparison red giant, α Tau, to minimize non–LTE effects. The CNO abundances are based on molecular lines from CO, OH, and CN.

The CNO abundances clearly show the effects of CN-processed material being dredged to the surface, while one MS giant shows an excess of ^{12}C, probably the result of He-burning products being dredged up during thermal pulses on the asymptotic giant branch (AGB).

The three MS giants studied all show enhancements of the s-process elements Sr, Y, Zr, Ba, and Nd. A range of integrated neutron exposures is evident with one star showing a large enhancement of Ba and Nd relative to Sr, Y, and Zr, while the other two show much lower enhancements of Ba and Nd. It is suggested that the MS stars are AGB stars and that their compositions reflect the addition of ^{12}C and s-process material from He-burning thermal pulses.

Subject headings: convection — stars: abundances — stars: late-type — stars: S-type

I. INTRODUCTION

Abundances of selected elements in red-giant stars offer clues to the nuclear processes occurring in the interiors of evolving stars and the mixing of matter between the deep interior and the spectroscopically observable surface. Changes in the surface composition of red giants as a function of evolutionary state and mass have been predicted (Becker and Iben 1979, 1980). Such predictions can be tested by spectroscopic analyses of the elemental abundances of real stars.

The atmospheres of MS and S stars certainly reveal evidence of contamination by neutron-irradiated material, as shown by a strengthening of lines of the primarily s-process element Zr (Boesgaard 1970). Some stars also contain Tc (Merrill 1952; Peery 1971), indicating that neutron irradiation and mixing have occurred recently. However, the literature contains very few thorough analyses of M and similar stars but a plethora of reports on G and K giants. This striking difference reflects the difficulties in obtaining spectra in regions clear of molecular blanketing and in finding suitable model atmospheres for these stars with severe molecular-line blanketing.

The key to the first problem is access to the near-infrared and infrared provided by modern detectors. Existence of windows between TiO bands in the near-infrared was exploited first by Yamashita and Utsumi (1962) in their curve of growth analysis of β Peg using lines drawn from the interval 8200–8800 Å. Recently, the infrared (1.5 to 4.0 μm) provided molecular lines for a determination of the C, N, and O abundances for the M supergiants α Ori (Lambert *et al.* 1984) and α Her (Tsuji 1984).

Problems created by the dearth of reliable model atmo-

spheres were revealed by Huggins' (1973) analysis of near-infrared Ti I and Fe I lines in a sample of K and M giants from K5 to M3. His analysis used scaled solar model atmospheres. The most striking result was the correlation between the derived metal abundances and the effective temperatures: metal deficiencies of -0.5 to -0.6 dex for M2 and M3 giants are an unlikely result for so common a star. Huggins suggested that this correlation arose because his model atmospheres did not reflect the structural changes induced by TiO line blanketing. Techniques for computing model atmospheres have now improved; for example, the model atmospheres for red giants computed by Johnson, Bernat, and Krupp (1980) take account of, by the method of opacity sampling, the molecular opacities of several important species, including CO and TiO.

Through quantitative spectroscopic analysis, the first (and second) dredge-up of the burning CN-cycle products has been studied extensively (Lambert and Ries 1981; Lambert 1981; Kjaergaard *et al.* 1982). M-type giants, which should have experienced this dredge-up via the giant's deep convective envelope, provide also the opportunity to probe the dredge-up of He-burning products on the asymptotic giant branch (AGB). Many of the M, MS, and S stars are near the luminosity at which thermal pulses and dredge-up of He-burning products are expected to occur. The evolution of thermally pulsing, AGB stars is extensively reviewed by Iben and Renzini (1983). MS and S stars may be living examples of AGB stars which are experiencing thermal pulses and varying degrees of mixing between interior and surface.

The importance of AGB evolution and mixing to stellar evolution, the synthesis of the elements, and the chemical evolution of the galaxy led us to investigate the chemical composition of stars of type M, MS, and S. The data are high-resolution, high signal-to-noise spectra in the near-IR and IR, providing a variety of molecular and atomic lines. These allow for the determination of abundances of carbon, nitrogen,

TABLE 1
BASIC STELLAR QUANTITIES

Star	Spectral Type[a]	$(V-K)$[b]	$M_v(K)$[c]	M_{Bol}[d]	Approximate Mass
α Tau	K5$^+$ III	3.67	0.0	−1.1	1.5
β Peg	M2$^+$ III	4.63	−0.1	−1.9	1.7
β And	M0$^+$ III	3.88	−0.8	−2.0	2.5
ν Vir	M1 III	3.95	−0.2	−1.7	2.0
δ Vir	M3$^+$ III	4.59	−0.4	−2.2	2.0
HR 5299	M4$^+$ III	5.57	−0.4	−3.1	2.0
HR 363	M3 IIS	e	...	−3.1^f	3.0
o^1 Ori	M3$^-$ IIIS	g	−1.1	−3.4	3.0
HR 6702	M5$^+$ II^h	6.21	−0.2	−3.4	2.5
30 Her	M6 III	7.02	−1.5	−5.5	4.0

  [a] Yamashita 1967.
  [b] Johnson et al. 1966.
  [c] Wilson 1976.
  [d] Bolometric correction using Bessell and Wood 1984.
  [e] $(R-I) = 1.25$.
  [f] Eggen 1972.
  [g] $(R-I) = 1.56$
  [h] Classified as M6 S by Jaschek et al. 1964. Yamashita 1967 notes YO enhanced.

oxygen, the $^{12}C/^{13}C$ ratio, and several of the elements up to the Fe peak and beyond. Our analysis utilizes the recent model atmospheres of Johnson, Bernat, and Krupp (1980). In the first paper, we examine nine M giants including a few MS giants.

II. OBSERVATIONS

High-resolution spectra of M giants were obtained using two instruments: the McDonald Observatory's 2.7 m telescope, coudé spectrograph, and Reticon array (Vogt, Tull, and Kelton 1978); and the Kitt Peak National Observatory's 4 m

telescope and Fourier transform spectrometer (FTS; Hall et al. 1978). Typical Reticon spectra have resolutions of 0.2 Å at λ7500, and the FTS spectra were obtained with a typical unapodized resolution of 0.05 cm^{-1} at 4500 cm^{-1}. In Table 1 we list the stars observed and basic data.

As the spectra of late-type stars are dominated by severe TiO blanketing in the visual, care was taken to observe in windows that are relatively free from TiO bands and telluric lines. In the near-IR accessible with the McDonald Reticon, two regions were chosen to provide atomic lines of key elements. The region from 7400–7580 Å is redward of the γ (0, 0) system of TiO and, from inspection of low-resolution ($\Delta\lambda = 10$ Å) spectrophotometric scans (Cochran 1978), should not be significantly depressed for spectral types earlier than M7 to M8. A second region near λ10000 was observed to be quite free from blanketing and provides additional atomic lines.

High-resolution IR spectra were obtained by us at KPNO with the FTS. Additional spectra were drawn from the KPNO archives. Two regions have been used for the results presented here, one near 1.6 μm and the other near 2.2 μm. Telluric-line contamination was removed by putting in ratio spectra of the program star and a hot star. Molecular lines from C-, N-, and O-bearing molecules are found in these regions. Near 1.6 μm we have used OH ($\Delta v = 2$) and CO ($\Delta v = 3$) vibration-rotation ($V - R$) lines, while near 2.2 μm we have CO ($\Delta v = 2$) (both ^{12}C and ^{13}C isotopes) $V - R$ lines and the CN ($\Delta v = 2$) red system ($A\,^2\Pi$–$X\,^2\Sigma$).

Figure 1 shows a sample McDonald spectrum near λ7550 for both an M an MS star. Note the stronger lines in the MS star due to the primarily s-process species Zr I and Y II. In Figure 2, we present a portion of an FTS spectrum for the MS star o^1 Ori in the region containing some of the CN lines used
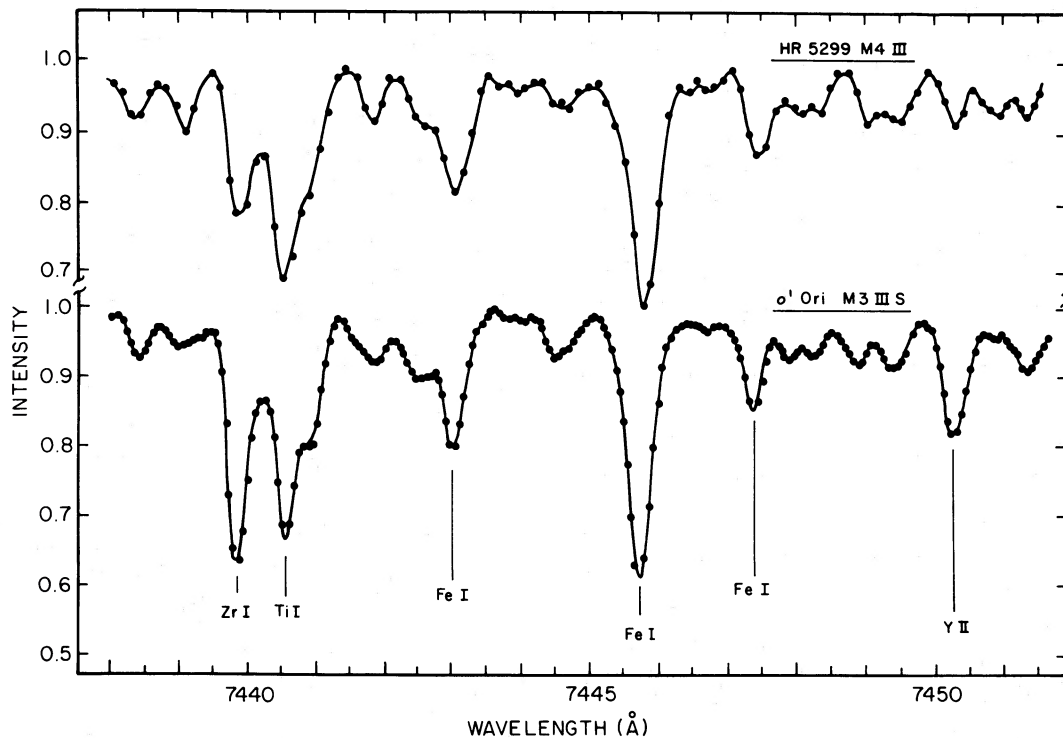
FIG. 1.—Sample McDonald Observatory Reticon spectra of both an M and an MS giant. The top spectrum was obtained with a Reticon array containing a smaller number of diodes.
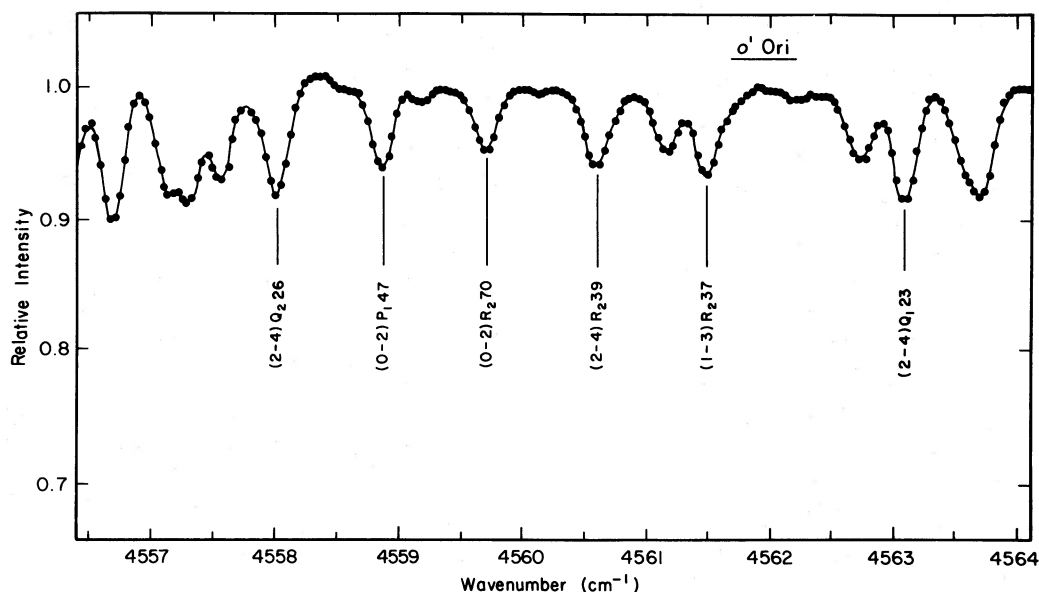
FIG. 2.—Sample FTS spectrum illustrating some of the fairly weak CN features

in this study. In both the near-IR and IR spectra, the continuum level is readily located. An adequate number of lines are well resolved, so that a great part of the analysis uses measurements of equivalent widths (W_λ). For selected problems involving the molecular bands, the analysis employed spectrum synthesis.

III. THE ABUNDANCE ANALYSIS

a) Model Atmospheres

Our abundance analysis combines the line list, line-blanketed model atmospheres, and a versatile program (Sneden 1974) for predicting equivalent widths and synthesizing selected spectral regions. Key and coupled challenges in the analysis are the determination of a star's surface gravity and an appearance of non–LTE effects.

Model atmospheres were taken from the grid computed by Johnson, Bernat, and Krupp (1980), who used the opacity-sampling technique to account for the line blanketing contributed by molecules including CO and TiO. Solar abundances were assumed. A model is matched to a star by considering the effective temperature (T_{eff}) and the surface gravity (g). Effective temperatures are from the ($V - K$) colors using the calibration provided by Ridgway *et al.* (1980) from angular diameters measured at lunar occultations. This calibration is in good agreement with that obtained from the infrared flux method (Tsuji 1981). For two stars, ($V - K$) colors are unavailable and the ($R - I$) colors were used to estimate T_{eff} using Tsuji's (1981) calibration. The uncertainty ΔT_{eff} would appear to be modest: $\Delta T_{eff} = \pm 100$ K.

Spectroscopists' traditional approach to the determination of g is to require that neutral and ionized lines of the same element yield the same abundance. This requirement defines a locus in the (T_{eff}, g) plane on which a point is isolated using an independent estimate of T_{eff}. An attempt to apply this method to M stars faces two difficulties: (1) a paucity of ionized lines from elements with an adequate number of neutral lines, and (2) departures from LTE in the excitation and ionization of the metals.

Our search for suitable ionized lines was almost fruitless.

Earlier, Yamashita (1965) reported an unsuccessful search of photographic spectra spanning the interval 5800–8900 Å. We located several Fe II lines from multiplets 72 and 73 near 7500 Å. These lines are strong enough and free from blending in only the earliest M stars. As a check on the non–LTE effects affecting the Fe I and Fe II lines, we used them to estimate the surface gravity of α Tau, our reference K5 giant. Three Fe II lines ($\lambda\lambda$7449.34, 7479.70, 7515.83) were measured in α Tau. Solar gf-values were derived for these lines (and the Fe I lines) based on equivalent-width measurements from the solar atlas of Delbouille, Neven, and Roland (1973), the solar atmosphere of Holweger and Müller (1974), and the iron abundance of Anders and Ebihara (1982). Enforcement of ionization equilibrium resulted in log $g = 0.8$. This is surely too low because with the effective temperature and absolute luminosity (obtained from α Tau's nearby distance of 18 pc), it yields a mass of $M \approx 0.3$ $M_\odot$, which is clearly too small. A mass of $M \approx 1.5$–2.0 $M_\odot$ is suggested by the location of α Tau in the H-R diagram (see below) and corresponds to log $g \approx 1.5 - 1.7$.

Our speculation is that iron is overionized relative to LTE. In the line-forming layers of a log $g = 1.5$ model, Fe$^+$ accounts for about 15% of the iron. If this fraction were raised to slightly more than 20%, the observed equivalent widths of the Fe II lines would be reproduced. This degree of overionization has only a modest influence on the Fe I lines. In detailed analyses of the K giants α Boo (Mäckle *et al.* 1975) and β Gem (Ruland *et al.* 1980), low-excitation lines of Fe I ($\chi \lesssim 3.5$ eV) yielded lower abundances than the high-excitation and ionized lines. Our selection of Fe I lines includes only high-excitation lines which may be little affected by departures from LTE.

This unsuccessful test of the Fe II lines in α Tau plus the fact that these lines are weak in the M giants (especially in the cooler stars, where blending is more severe) encouraged us to compute surface gravities from masses estimated from evolutionary tracks and the H-R diagram. Absolute luminosities are provided by the absolute visual magnitudes, $M_v(K)$, obtained via the Wilson-Bappu effect (Wilson 1976) and the bolometric corrections from Bessell and Wood (1984). Table 1 gives the adopted values of $M_v(K)$ and M_{bol}. Using our estimated effec-
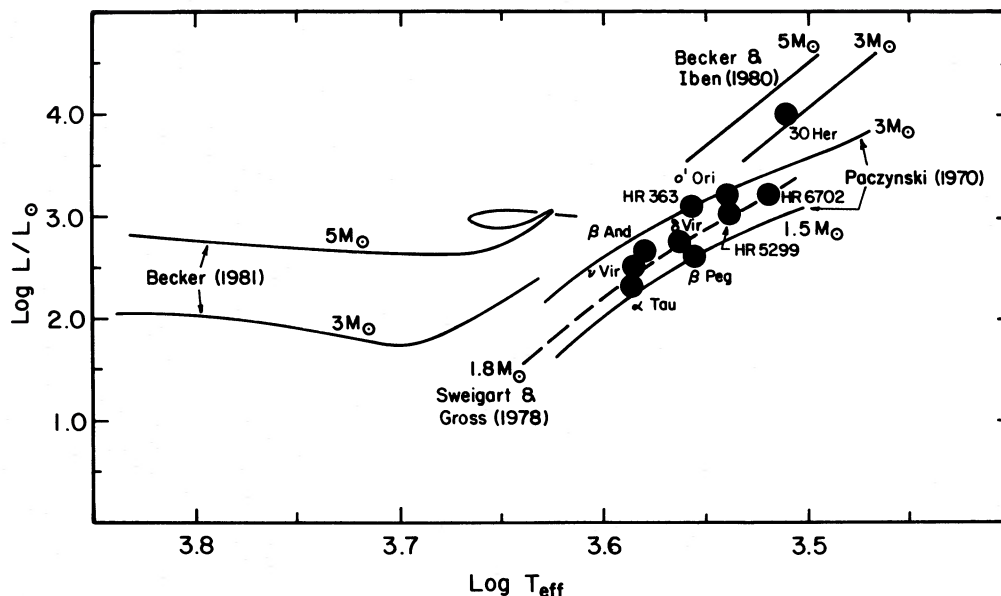
FIG. 3.—Model evolutionary tracks of different-mass stars from several investigators are shown along with the derived luminosities and effective temperatures of the red giants in this study.

tive temperatures and luminosities, we plot in Figure 3 the stars in a log $L/L_\odot$–log T_{eff} plane along with three sets of theoretical evolutionary tracks. Models by Becker (1981) depict evolution to the beginning of the first ascent, while those of Becker and Iben (1980) are for AGB stars undergoing thermal pulses. The tracks by Paczyński (1970) and Sweigart and Gross (1978) are for first-ascent giants. All models plotted are for solar metallicity and a helium abundance $Y = 0.25$. Figure 3 cannot be used to define a star's evolutionary status uniquely because the asymptotic giant branch, at the lower luminosities, parallels and overlaps the first giant branch. However, one suggestion from such a diagram is clear: this particular sample of stars, picked on the basis of their luminosity classification as giants and their low level of variability, are low-to-intermediate-mass stars ($M \approx 1$–$3\ M_\odot$). Errors in T_{eff} of 200 K will change log T_{eff} by only 0.025 and uncertainties in $M_v(K)$ of one magnitude will change log $L/L_\odot$ by 0.4. We show models from several investigators to emphasize the general agreement between their various models. Masses in the range of 1–3 $M_\odot$ are not surprising for this sample of stars, as pointed out by Scalo, Dominy, and Pumphrey (1978), who estimate that the typical field red giant should have a mass of roughly 1–1.5 $M_\odot$.

The estimated masses, as derived from the evolutionary tracks, are listed in Table 1. The surface gravity for a particular star g_* can be estimated from the standard relation

$$\log g_*/g_\odot = \log (M_*/M_\odot) - \log (L_*/L_\odot) + 4 \log (T_*/T_\odot) .$$

Inspection of the evolutionary tracks in Figure 3 suggests that, for this sample of stars, our masses are unlikely to be in error by as much as a factor of 2 so that, for a given luminosity and effective temperature, g is defined to within approximately 0.3 dex.

b) The Metal Abundances

Departures from LTE are of concern in the analysis of the atomic lines. Recent studies (Ruland et al. 1980; Tomkin, and Lambert 1983) have shown that the assumption of LTE in

late-type giants can lead to erroneous abundances. However, the non–LTE effects diminish for high-excitation lines (formed at deeper layers) from the dominant stage of ionization for a particular species. Furthermore, when a differential analysis is conducted using a comparison star of similar T_{eff} and surface gravity, the non–LTE effects largely disappear; see for example, Tomkin and Lambert's (1983) analysis of the classical Ba II star HR 774 and the standard star β Gem. Here, abundances based upon atomic lines will be referenced to α Tau, a K5 giant. Kovács (1983a) has presented a detailed abundance analysis of α Tau and finds that for the Fe-peak and heavier elements (up to the Ba group) the distribution is solar to within the uncertainties of the analysis (roughly ± 0.2 dex). The non–LTE effects are seen in the Mn I and Ni I lines in α Tau, but the effects are not large. There is a hint that the Fe-peak abundances may be slightly underabundant relative to solar (~ 0.05–0.1 dex).

Table 2 is a list of the atomic lines used in the near-IR along with their measured equivalent widths in the stars. All the abundances derived from these lines will be set in ratio to α Tau, so the gf-values are not a relevant ingredient; however, a few words concerning them are in order. As with the Fe I lines, the Ni I and Ti I lines are visible in the solar spectrum; hence, solar gf-values were derived. The heavy-element lines are not all detectable in the Sun; hence the gf-values as given in Kurucz and Peytremann (1975) were employed.

Few species are represented by lines so weak that saturation is unimportant; hence, the microturbulence must be derived. The microturbulent velocity ξ was determined from the Fe I, Ni I, and Ti I lines by demanding that the abundances be independent of equivalent width. Figure 4 shows a typical determination of ξ for the star β And. Values of ξ derived from the three sets of lines are consistent: we estimate an uncertainty, at most, of $\Delta \xi \approx +0.3$ km s^{-1} to be representative. Table 3 contains the derived quantities T_{eff}, log g, and ξ for our sample of giants.

We have estimated uncertainties in our derived abundances in two ways. First, we compute the standard deviations of the

TABLE 2
ATOMIC LINE LIST

SPECIES	λ (Å)	χ (eV)	log gf	W_λ (mÅ)									
				α Tau	β Peg	β And	δ Vir	ν Vir	HR 5299	o^1 Ori	HR 363	30 Her	HR 6702
Ti I	7337.78	2.24	−1.37	74	91	80	116	75	125	82	80	...	...
	7474.94	1.75	−1.98	91	105	96	123	96	128	105	98	123	127
	7496.12	2.24	−0.88	114	119	104	138	102	125	115	111	143	160
	9997.94	1.87	−1.62	105	125	...	126	105	133	138	105	157	147
	10003.02	2.15	−1.26	100	98	...	113	95	112	119	94	150	118
	10034.55	1.45	−2.01	140	180	...	170	147	187	190	168	232	225
Fe I	7418.67	4.14	−1.54	100	94	93	112	91	110	87	80	...	75
	7447.43	4.95	−0.97	71	58	59	74	67	55	57	41	74	63
	7454.02	4.19	−2.43	61	47	51	64	53	60	53	39	79	58
	7478.87	3.37	−3.84	43	32	34	48	29	36	46	33	...	...
	7507.30	4.41	−0.93	113	95	105	118	87	104	96	88	101	117
	7559.68	5.06	−0.96	67	44	60	68	45	51	...	...	44	48
	7583.80	3.02	−1.97	175	171	176	173	170	182	160	157	185	178
	10065.08	4.81	−0.68	85	68	...	67	75	75	74	60	59	71
Ni I	7385.24	2.74	−1.73	122	120	124	131	122	125	115	98	115	120
	7393.63	3.61	+0.03	146	134	144	162	147	148	131	116	157	145
	7414.51	1.99	−1.97	187	182	176	201	180	203	175	160	232	216
	7422.30	3.63	−0.03	153	140	141	168	146	163	143	131	141	166
	7522.78	3.66	−0.30	160	129	140	171	145	161	132	121	149	160
	7525.14	3.63	−0.51	125	103	120	126	113	116	115	97	90	115
	7574.08	3.83	−0.49	106	101	113	120	101	128	101	91	116	116
Sr II	10036.65	1.80	−1.31	122	134	...	122	130	167	189	200	192	211
Y II	7450.32	1.74	−1.88	53	33	42	30	35	34	71	68	47	55
Zr I	7439.89	0.54	−1.81	99	89	82	99	97	95	148	137	113	116
	7553.00	0.51	−2.71	44	24	30	...	28	51	66	70	57	78
	7554.73	0.51	−2.28	75	74	72	82	71	100	127	119	...	...
	7558.41	1.54	−1.47	26	20	26	23	18	30	44	48	32	41
Ba I	7392.41	1.57	+0.09	15	20	24	23	22	28	40	47	30	28
Nd II	7513.73	0.92	−1.18	22	22	25	32	23	39	42	85	56	51

abundances, derived on a line-by-line basis, from those species represented by more than one or two lines. This gives a measure of how consistent a set of measured equivalent widths is for a given model atmosphere. These uncertainties, of course,

give no direct information on the sensitivity of abundance to the particular parameters of the model atmosphere.

The sensitivity to the model atmospheres was assessed by changing the atmospheric parameters over a plausible range of $T_{\rm eff}$, log g, and ξ. This procedure was carried out over the range of temperatures, gravities, and microturbulent velocities found in our stars. The change in the abundance created by varying each atmospheric quantity was determined and is listed in Table 4. This is a compilation for two temperatures: $T_{\rm eff} = 3300$ K and $T_{\rm eff} = 3700$ K. The differences were computed using equivalent widths that are representative of those in the stars. Note that over this range of temperatures, the sensiti-
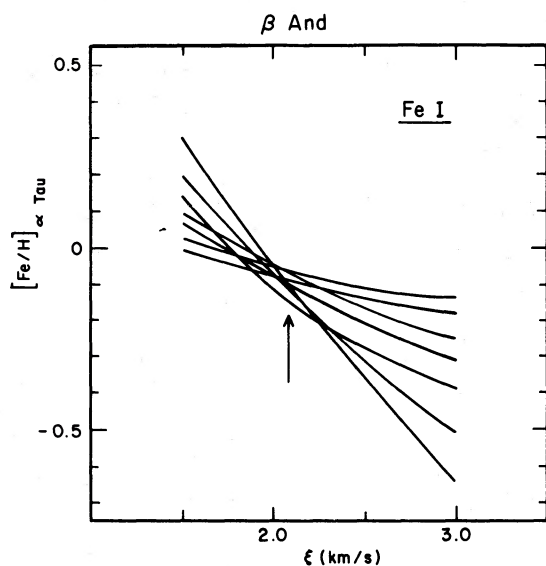
FIG. 4.—Derivation of the microturbulent velocity for β And using seven Fe I lines. The arrow indicates the value of ζ used for β And.

TABLE 3
DERIVED STELLAR PROPERTIES

Star	$T_{\rm eff}$	log g	ξ (km s^{-1})
α Tau	3850	1.5	1.9
β Peg	3600	1.2	2.0
β And	3800	1.6	2.1
ν Vir	3750	1.5	2.0
δ Vir	3650	1.3	2.3
HR 5299	3450	0.9	2.6
HR 363	3600	1.0	1.8
o^1 Ori	3450	0.8	2.0
HR 6702	3300	0.7	2.5
30 Her	3250	0.2	2.7

TABLE 4

DEPENDENCE OF DERIVED ABUNDANCE ON MODEL ATMOSPHERE PARAMETERS

		$T_{eff} = 3700$ K, log $g = 1.0$, $\xi = 2.2$ km s^{-1}			$T_{eff} = 3300$ K, log $g = 0.7$, $\xi = 2.5$ km s^{-1}		
Species	log (W/λ)	$\Delta\xi = +0.3$ km s^{-1}	Δ log $g = +0.3$	$\Delta T = +100$ K	$\Delta\xi = +0.3$ km s^{-1}	Δ log $g = +0.3$	$\Delta T = +100$ K
CO	-4.90	-0.08	$+0.10$	$+0.03$	-0.08	$+0.12$	$+0.06$
OH	-4.85	-0.04	$+0.02$	$+0.20$	-0.04	-0.01	$+0.16$
CN	-5.40	-0.04	$+0.14$	-0.05	-0.03	$+0.14$	-0.06
Fe I	-4.95	-0.10	$+0.10$	-0.12	-0.10	$+0.10$	-0.02
Ni I	-4.75	-0.16	$+0.09$	-0.10	-0.16	$+0.10$	$+0.04$
Ti I	-4.85	-0.10	$+0.05$	$+0.08$	-0.10	$+0.07$	$+0.09$
Sr II	-4.75	-0.18	$+0.12$	-0.05	-0.17	$+0.10$	$+0.08$
Y II	-5.15	-0.06	$+0.26$	-0.23	-0.07	$+0.24$	-0.17
Zr I	-4.90	-0.10	-0.22	-0.13	-0.14	$+0.20$	-0.09
Ba I	-5.25	-0.03	$+0.01$	$+0.10$	-0.02	$+0.01$	$+0.11$
Nd II	-5.25	-0.02	$+0.13$	-0.03	-0.04	$+0.12$	-0.01

vities of the derived abundances from each species are similar for different model atmospheres; ie., the ratio [X/Fe][2] is, in general less sensitive than [X/H] to the atmosphere parameters. Also note that we have included sensitivities for the C-, N-, and O-bearing molecules CO, CN, and OH. We will discuss the C, N, and O abundances in the next section.

Table 5 contains the final abundances for the ten stars. For completeness, we include the C, N, and O abundances and will discuss their derivation in the next section. The listed errors are the standard deviations from these species where we had more than one line. These standard deviations can be compared to the sensitivity of abundance to model-atmosphere quantities listed in Table 4. In general, errors encurred due to uncertainties in the model atmosphere tend to be larger than the internal consistency in a sample of lines.

Other sources of error are at present impossible to quantify. The leading contributor of a systematic error is probably our assumption that non–LTE effects in the excitation and ionization of the metals cancel when the M stars are analyzed with respect to the K5 giant α Tau. Inspection of Table 5 shows that this error may be small. For example, [X/Fe] taken with respect to α Tau is −0.11 (Ti), −0.15 (Ni), +0.14 (Sr), +0.12 (Y), +0.21 (Zr), −0.04 (Ba), and +0.23 (Nd) for HR 5299, one of the cooler members of the sample. The coolest star of

[2] We adopt the standard notation $[X] = \log_{10} (X)_{program\,star} - \log_{10} (X)_{comparison\,star}$.

normal composition according to its spectral classification is 30 Her, for which [X/Fe] shows slightly larger than expected differences from the expected null value: −0.38 (Ti), −0.25 (Ni), +0.25 (Sr), +0.26 (Y), +0.34 (Zr), −0.29 (Ba), and +0.13 (Nd). The TiO–line blanketing of the 7400–7580 Å region, which is noticeably stronger in 30 Her than in earlier M giants, must be a contributor to the larger scatter of the [X/Fe] values about zero. The unweighted mean is small: [X/Fe] = +0.08 and not significantly different from the similar mean, [X/Fe] = +0.06, for HR 5299.

An expectation that the null result [X/Fe] = 0.0 should be recoverable in the absence of systematic errors is based on two obvious assumptions. First, we must assume that the null result applies to the original composition of the star, i.e., the element-by-element distribution is the same as the comparison star α Tau. Second, we assume that a star classed as "normal" after spectral classification has normal abundances of the s-process elements. However, if s-process enrichment occurs in small increments, quantitative spectroscopy at high dispersion will surely detect much smaller enrichments than are detectable by spectral classification. Hence, some normal M stars may show modest enrichments of Sr through Nd. We conclude that the differential analysis relative to α Tau has reduced systematic errors to an insignificant level.

In the atmosphere of an M giant, metallic oxides reduce the partial pressure of free atoms and ions. Molecular (LTE) equilibrium is treated correctly in the program LINES. In addition

TABLE 5

STELLAR ABUNDANCES[a]

Element	α Tau	β Peg	β And	δ Vir	υ Vir	HR 5299	o^1 Ori[b]	HR 363[b]	30 Her[b]	HR 6702[b]
^{12}C	$8.38 \pm .08$	$+8.45 \pm .06$	$+8.53 \pm .08$	$+8.53 \pm .09$	$+8.52 \pm .09$	$+8.46 \pm .07$	$+8.55 \pm .09$	$+8.75 \pm .09$	$+8.32 \pm .08$	$+8.52 \pm .09$
^{12}C/^{13}C	10	8	12	13	12	10	26	17	12	14
^{14}N	$8.35 \pm .06$	$+8.26 \pm .06$	$+8.37 \pm .08$	$+8.28 \pm .08$	$+8.33 \pm .08$	$+8.40 \pm .10$	$+8.49 \pm .06$	$+8.27 \pm .10$	$+8.55 \pm .05$	$+8.60 \pm .07$
^{16}O	$8.77 \pm .08$	$+8.82 \pm .06$	$+8.84 \pm .06$	$+8.78 \pm .06$	$+8.91 \pm .06$	$+8.71 \pm .07$	$+8.80 \pm .05$	$+8.99 \pm .05$	$+8.76 \pm .08$	$+8.78 \pm .06$
[Ti/H]α Tau	0.00	$-0.07 \pm .10$	$-0.07 \pm .12$	$+0.16 \pm .20$	$0.00 \pm .17$	$-0.14 \pm .14$	$-0.25 \pm .14$	$-0.15 \pm .13$	$-0.31 \pm .10$	$-0.27 \pm .13$
[Fe/H]α Tau	0.00	$-0.11 \pm .13$	$-0.10 \pm .11$	$+0.06 \pm .17$	$-0.09 \pm .20$	$-0.03 \pm .21$	$+0.02 \pm .1$	$-0.15 \pm .18$	$+0.07 \pm .22$	$+0.02 \pm .21$
[Ni/H[α Tau	0.00	$-0.14 \pm .12$	$-0.10 \pm .16$	$+0.11 \pm .12$	$-0.02 \pm .08$	$-0.18 \pm .21$	$-0.09 \pm .21$	$-0.09 \pm .18$	$-0.17 \pm .22$	$-0.01 \pm .20$
[Sr/H]α Tau	0.00	$+0.11$	...	-0.10	$+0.26$	$+0.11$	$+0.62$	$+0.85$	$+0.32$	$+0.66$
[Y/H]α Tau	0.00	-0.13	$+0.03$	-0.13	$+0.03$	$+0.09$	$+0.75$	$+0.58$	$+0.33$	$+0.64$
[Zr/H]α Tau	0.00	$+0.02 \pm .17$	$+0.04 \pm .13$	$+0.14 \pm .10$	$+0.10 \pm .20$	$+0.18 \pm .12$	$+0.80 \pm .22$	$+0.73 \pm .18$	$+0.41 \pm .09$	$+0.57 \pm .11$
[Ba/H]α Tau	0.00	-0.08	$+0.21$	$+0.02$	$+0.10$	-0.07	$+0.30$	$+0.52$	-0.22	-0.18
[Nd/H]α Tau	0.00	-0.16	$+0.06$	$+0.19$	$+0.01$	$+0.20$	$+0.20$	$+0.65$	$+0.20$	$+0.19$

[a] Absolute abundances are scaled to log ε(H) = 12.0. On this scale the solar CNO abundances are log ε(C) = 8.67, log ε(N) = 7.99, log ε(O) = 8.92 (Lambert 1978).
[b] MS or MS-like stars.

to molecules affecting the partial pressures of C, N, and O, we included the following oxides, TiO, SrO, YO, ZrO, BaO and NdO. Equilibrium constants were taken from Tsuji (1973). A source of uncertainty is the dissociation energy $D_0{}^0$. We list in Table 6 the $D_0{}^0$'s adopted by Tsuji (1973) and compare these values with the latest recommended values from a critical review of the available data (Pedley and Marshall 1983). Tsuji's values fall within the estimated uncertainty ($\Delta D_0{}^0$) of these latest recommendations except for ZrO, BaO, and NdO. Test calculations were run to estimate the effect on the metal abundances of a change in $D_0{}^0$ to the new recommended values. In a few cases, incomplete knowledge of the electronic structure introduces a modest uncertainty into the molecular partition function, but the uncertainty is insignificant relative to that contributed by $\Delta D_0{}^0$. The effect on the derived abundances of $\Delta D_0{}^0$ is insignificant except for Zr in the very coolest stars

TABLE 6

DISSOCIATION ENERGIES OF METALLIC OXIDES
(eV)

Oxide	Tsuji 1973	Pedley & Marshall 1983
TiO	6.83	6.92 ± 0.10
SrO	4.21	4.37 ± 0.17
YO	7.58	7.44 ± 0.12
ZrO	8.37	8.00 ± 0.14
BaO	5.44	5.78 ± 0.14
NdO	7.50	7.24 ± 0.13

($T_{\rm eff} \lesssim 3300$ K). At $T_{\rm eff} = 3200$ K and log $g = 0.5$, adoption of the new value of $D_0{}^0 = 8.00$ eV for ZrO reduces the Zr abundance by 0.25 dex. This uncertainty in $D_0{}^0$ for ZrO may mean that our derived Zr abundances for 30 Her and HR 6702 are a bit large; however, the neighboring elements Sr and Y are unaffected, and hence our conclusions are not altered in any significant way.

c) Carbon, Nitrogen, and Oxygen

Our approach to the C, N, and O abundances is to derive absolute abundances for α Tau and the M giants. With one possible exception—the dissociation energy of CN—the necessary basic molecular data are of sufficient accuracy. LTE is expected to apply to the vibration-rotation transitions of CO and OH (Thompson 1973; Hinkle and Lambert 1975), and departures from LTE affecting the infrared bands of CN A $^2\Pi$–X $^2\Sigma^+$ electronic transition should be small (Hinkle and Lambert 1975; Lambert et al. 1984). A third factor motivating us to analyze the M stars without a direct scaling to α Tau was the odd N abundance for α Tau obtained earlier by Lambert and Ries (1981): [N/Fe] = -0.20, but the mean value for ~ 20 G and K giants was [N/Fe] = $+0.40$.

A summary of the adopted basic molecular data suffices because Lambert et al. give a detailed discussion as part of a C, N, and O analysis of the M supergiant α Ori. A few revisions are noted here. A search of the spectra provided the list of $^{12}C^{16}O$ (hereafter CO) lines given in Table 7 along with their equivalent widths (W_σ). Chackerian and Tipping (1983) provide

TABLE 7

^{12}CO LINE LIST

BAND	LINE	σ (cm^{-1})	χ (eV)	log gf	α Tau	β Peg	β And	δ Vir	ν Vir	HR 5299	o^1 Ori	HR 363	30 Her	HR 6702
										W_σ (cm^{-1})				
3–0	P36	6147.00	0.32	−7.88	0.032	0.044	0.030	0.047	...	0.063	0.054	0.054	0.069	0.074
4–1	P19	6181.02	0.36	−7.47	0.047	0.060	0.044	0.070	0.049	0.085	0.067	0.069	0.081	0.089
	P18	6186.70	0.35	−7.49	0.045	0.061	0.039	0.075	0.043	0.077	0.068	0.075	0.085	0.094
5–2	P14	6129.82	0.58	−7.16	0.038	0.056	0.039	0.068	0.057	0.067	0.071	0.074	0.074	0.079
	P13	6134.95	0.57	−7.19	0.034	0.055	0.037	0.062	0.052	0.074	0.067	0.080	0.070	0.083
	P10	6149.71	0.55	−7.29	0.034	0.052	0.038	...	0.046	0.071	...	0.066	...	0.083
6–3	R63	6127.88	1.71	−5.80	...	...	0.023	...	0.040	...	0.036	0.049	0.044	....
	R60	6137.37	1.63	−5.84	0.034	0.048	0.036	0.065	0.037	...	0.061	0.076	...	0.078
	R59	6140.30	1.60	−5.85	0.032	0.045	0.030	0.057	0.048	0.054	0.058	0.071	0.059	0.070
	R41	6173.79	1.18	−6.09	0.049	0.067	0.054	0.072	0.064	0.085	0.082	0.077	0.080	0.089
	R20	6167.39	0.88	−6.50	0.058	0.073	0.066	0.092	0.071	0.083	0.089	0.094	...	0.104
	R18	6164.28	0.87	−6.55	0.051	...	0.055	0.090	0.061	0.076	0.085	0.092	...	0.110
	R17	6162.56	0.86	−6.58	0.051	0.071	0.051	0.093	0.055	0.080	0.088	0.091	0.087	0.104
	R16	6160.73	0.85	−6.61	0.058	0.073	0.057	0.098	...	0.080	0.089	0.092	0.088	0.103
	R15	6158.79	0.84	−6.64	0.050	0.066	0.050	0.091	0.067	0.085	0.084	0.088	0.088	0.100
	R14	6156.75	0.84	−6.67	0.048	0.067	0.049	0.091	0.054	0.077	0.074	0.084	0.091	0.098
	R8	6142.25	0.80	−6.92	0.034	0.049	0.034	0.064	0.047	0.067	0.057	0.074	0.072	0.077
	R6	6136.56	0.80	−7.04	0.034	0.049	0.036	0.061	0.044	0.052	...	...	0.069	0.076
	R4	6130.45	0.79	−7.20	0.018	0.034	0.015	0.047	0.025	...	0.039	0.047	0.049	0.056
2–0	R94	4285.21	2.07	−4.84	0.039	0.038	...	0.034	...	0.042	...	...	...	...
	R92	4292.04	1.98	−4.85	0.038	0.033	0.039	0.040	0.035	0.048	0.054	0.055	0.049	0.052
	R81	4323.69	1.55	−4.93	0.053	0.057	0.059	0.060	0.058	0.070	0.071	0.069	0.067	0.080
	R80	4326.07	1.51	−4.94	0.057	0.062	0.063	0.068	0.065	0.071	0.071	0.073	...	...
	R79	4328.37	1.48	−4.95	0.057	0.067	0.065	0.070	0.066	0.073	0.075	0.077	0.080	0.086
	R78	4330.58	1.44	−4.95	0.057	0.072	0.068	0.069	0.066	0.077	0.077	0.072	0.085	0.090
	R77	4332.72	1.40	−4.96	0.058	0.069	0.065	0.076	0.068	0.075	0.070	0.077	...	0.095
3–1	R63	4299.00	1.21	−4.61	0.084	0.093	0.096	0.086	0.091	0.108	0.113	...	0.135	0.126
	R37	4298.74	0.60	−4.90	0.104	0.128	0.135	0.127	...	0.170	0.168	...	0.219	0.225
	R32	4292.75	0.51	−4.98	0.108	0.134	0.128	0.140	0.127	0.173	0.177	...	...	...

TABLE 8

OH Line List

Band	Line	σ (cm^{-1})	χ (eV)	log gf	W_σ (cm^{-1})									
					α Tau	β Peg	β And	δ Vir	ν Vir	HR 5299	o^1 Ori	HR 363	30 Her	HR 6702
2–0	$P_1 + 21.5$	5680.60	1.01	−4.90	0.045	0.085	0.066	0.073	0.073	0.093	0.094	0.088	...	0.097
	$P_1 − 21.5$	5683.44	1.01	−4.90	0.047	0.092	0.063	0.079	0.074	0.087	0.086	0.093	...	0.105
	$P_2 + 19.5$	5767.44	0.93	−4.97	0.062	0.086	0.072	0.089	0.086	0.091	0.088	0.100	0.140	0.110
	$+ 20.5$	5682.68	1.02	−4.94	0.055	0.083	0.069	0.079	0.082	0.095	0.086	0.095	...	0.098
	$P_1 − 18.5$	5848.22	0.84	−5.01	0.064	0.102	0.073	0.091	0.096	0.107	0.091	...	0.133	0.121
3–1	$P_1 + 15.5$	5842.85	0.96	−4.64	0.091	0.126	0.100	0.104	0.111	0.133	0.114	0.140	0.166	0.147
	$P_1 − 15.5$	5844.75	0.96	−4.64	0.079	0.110	...	0.092	0.099	0.116	0.102	0.125	...	0.126
	$P_2 + 16.5$	5700.69	1.10	−4.60	0.071	...	0.089	0.097	0.091	0.103	0.102	0.120	0.138	0.127
	$P_2 − 14.5$	5847.59	0.96	−4.69	0.060	0.118	0.078	0.089	0.096	0.106	0.093	0.115	0.130	0.118
	$− 16.5$	5702.30	1.10	−4.60	0.060	0.105	0.076	0.087	0.081	0.100	0.096	0.109	0.124	0.114
4–2	$P_1 + 12.5$	5737.69	1.19	−4.47	0.054	0.084	0.065	0.078	0.083	0.092	0.080	0.086	...	0.095
	$P_1 − 12.5$	5736.26	1.19	−4.47	0.055	0.078	0.073	0.074	0.089	0.091	0.083	0.091	...	0.092
	$P_2 + 9.5$	5863.48	1.10	−4.65	0.061	0.102	0.072	0.087	0.094	0.101	0.091	...	0.135	0.120
	$+ 10.5$	5802.94	1.15	−4.59	0.075	0.106	0.084	0.102	0.094	0.093	0.092	0.103	0.164	0.130
	$P_2 − 9.5$	5862.75	1.10	−4.65	0.066	0.105	...	0.087	0.094	0.107	0.096	0.110	...	0.120
	$− 10.5$	5803.79	1.15	−4.59	0.090	0.115	...	...	0.115	...	0.115	0.125	...	0.145
5–3	$P_1 + 4.5$	5840.04	1.31	−4.86	0.031	0.059	0.043	0.048	0.061	0.076	0.060	0.076	0.102	0.080
	$+ 6.5$	5752.78	1.35	−4.65	0.035	0.061	...	0.064	0.071	0.053	0.061	0.070	0.095	0.077
	$+ 7.5$	5704.35	1.38	−4.56	0.040	0.061	0.048	0.056	0.059	0.066	0.074	0.69	...	0.073
	$P_1 − 6.5$	5752.15	1.35	−4.65	0.032	0.063	0.046	0.056	0.059	0.065	0.055	0.072	0.096	0.077
	$− 7.5$	5705.01	1.38	−4.56	...	0.075	...	...	0.061	...	0.058	...	...	0.090
	$P_2 − 6.5$	5714.06	1.39	−4.65	0.050	0.072	0.062	0.073	0.067	0.077	0.065	0.092	0.099	0.092

recipes for computing accurate gf-values. Spectrum synthesis of a window encompassing the 2–0 $^{13}C^{16}O$ band head provided the ^{13}C abundance in the hotter stars. The line list for this synthesis includes all significant contributions from the $^{12}C^{16}O$, $^{13}C^{16}O$, $^{12}C^{17}O$, and $^{12}C^{18}O$ first-overtone bands as well as the weak lines provided by the CN red system ($\Delta V = -2$) bands. In the cooler stars ($T_{eff} < 3400$ K) the band head becomes too strong to be a reliable abundance indicator and equivalent widths were measured from weak, unblended $^{13}C^{16}O$ lines taken from the line list used by Dominy, Hinkle, and Lambert (1984).

Frequencies of first-overtone V–R transitions from the OH $^2\Pi$ ground state were measured by Maillard, Chauville, and Mantz (1976) with additional lines predicted from a set of $^2\Pi$ energy levels (Beer 1974). Table 8 gives the selected lines with their W_σ's. Lambert et al. (1984) concluded that the published experimental results on the transition probabilities of the V–R transitions were of inferior accuracy to the theoretical predic-

tions from quantum calculations. With the publication of new ab initio calculations (Werner, Rosmus, and Reinsch 1983), the theoretical estimates have further improved in accuracy. Grevesse, Sauval, and van Dishoeck (1985) analysed solar V–R OH lines to show that the electric dipole moment function (EDMF) computed by Werner et al. provides the best fit to the run of the solar W_σ's within the 1–0 and 2–1 bands. A similar conclusion was drawn from an analysis of solar pure-rotation OH lines (Sauval et al. 1984). Van Dishoeck (1984) provided transition probabilities for OH V–R line predictions combining Werner et al.'s EDMF with an accurate potential energy curve. These predictions lead to the gf-values listed in Table 8 and supersede the values adopted by Lambert et al. (1984). The newer values result in a slight increase in the O abundance.

A selection of the many CN red-system lines around 2 μm was made (Table 9) from a region virtually free of telluric lines. The gf-values are computed from ab initio calculations of the band f-values (Larsson, Siegbahn, and Ågren 1983). Recent

TABLE 9

CN Line List

Band	Line	σ (cm^{-1})	χ (eV)	log gf	W_σ (cm^{-1})									
					α Tau	β Peg	β And	δ Vir	ν Vir	HR 5299	o^1 Ori	HR 363	30 Her	HR 6702
0–2	$P_1 47$	4558.98	1.02	−2.27	0.007	0.008	0.006	...	0.007	0.010	0.014	0.013	0.013	0.016
	$P_2 24$	4586.53	1.00	−2.29	0.010	0.011	0.010	0.013	0.011	0.012	0.019	0.016	...	0.017
	$Q_1 57$	4563.90	1.26	−1.70	0.009	0.010	0.010	0.011	0.010	...	0.021	...	0.016	...
1–3	$Q_2 44$	4567.15	1.20	−1.69	0.012	0.013	0.012	0.015	0.013	...	0.022	0.020	0.020	....
	$Q_2 45$	4553.77	1.22	−1.68	0.013	0.011	0.007	...	0.012	0.013	0.022	0.020	...	0.019
2–4	$Q_1 19$	4587.28	1.08	−1.90	0.012	...	...	0.013	0.012	0.015	...	0.021	...	0.019
	$Q_1 23$	4563.16	1.12	−1.81	0.012	0.011	0.012	0.011	0.011	0.010	0.021	0.023	0.017	0.020
	$Q_2 26$	4558.03	1.15	−1.77	0.012	0.010	0.010	0.011	0.010	0.013	0.019	0.021	0.016	0.019
	$R_2 39$	4560.60	1.34	−1.86	0.007	0.007	0.008	0.006	0.009	0.008	0.015	...	0.012	0.012

measurements (Taherian and Slanger 1984; Nishi, Shinohara, and Hanazaki 1982) of the radiative lifetimes of the $A\ ^2\Pi$ state are in good agreement with the *ab initio* predictions. The adopted *gf*-values should have an accuracy of $\pm 10\%$.

All analyses of CN lines are affected adversely by the continuing uncertainty about the CN dissociation energy—see Lambert *et al.* (1984). We adopt $D_0^0 = 7.60$ eV and consider how the abundances are affected by a ± 0.1 eV uncertainty. Over the range of temperatures in our sample, $\partial[\log \epsilon(N)]/\partial D_0^0 = -0.13$ to -0.15 per 0.10 eV.

IV. DISCUSSION

a) Introduction

In the following section we discuss (1) the Fe-peak elements, (2) C, N, and O—a trio monitoring the admixture of hydrogen- and helium-burning products in the atmosphere, (3) the heavy, s-process elements, and (4) the evolutionary status of the MS stars.

b) The Iron Peak

Results in the form [X/H] are summarized in Table 5 where we assume [X/H] = 0.0 for α Tau. It is clear that our analysis, for the first time, provides plausible results for the metallicity of M giants. If [Fe/H] is taken as the metallicity index, the range for the sample of nine M or MS giants is -0.11 to $+0.06$ dex. This range is quite consistent with the metallicity distribution for stars in the local neighborhood; for example, Tinsley (1980) notes that samples of main-sequence stars provide a mean metallicity [Fe/H] = -0.2 dex with a dispersion $\sigma = 0.2$ dex after correction for observational errors. This contrasts sharply with Huggins' (1973) analysis reporting that the cooler M giants were quite metal-poor; for example [Fe/H] = -0.46 for β Peg and -0.30 for δ Vir where the comparison star α Boo was assumed to correspond to [Fe/H] = -0.47. If one adopts [Fe/H] = -0.70, as determined by Mäckle *et al.* (1975; see also Bell, Edvardsson and Gustafsson 1984), Huggins' metallicities must be reduced by 0.24 dex. It is unlikely that these stars, typical M giants, can have a metallicity almost as low as that of Arcturus. Huggins suspected that an analysis using appropriately line-blanketed model atmospheres would return near-solar metallicities for these bright M giants. Our results fully confirm his suspicions.

Inspection of Table 5 shows that [Ti/H] is correlated with the effective temperature dropping from [Ti/H] ≈ 0 at 3800 K to -0.3 at 3300 K. This correlation points to a systematic error affecting the analysis of the low-excitation Ti I lines. No correlation is seen for [Fe/H] or [Ni/H] based on Fe I and Ni I

lines of higher excitation potential: mean values are χ (Fe I) = 4.2 eV, χ (Ni I) = 3.3 eV, but χ (Ti I) = 2.0 eV. Ruland *et al.* (1980) showed that the low-excitation lines of neutral species in the K giants β Gem gave systematically lower abundances when LTE was assumed. It is a plausible extrapolation to assume that these departures from LTE are magnified in the cooler giants and that they are not completely removed in a differential analysis with respect to α Tau.

c) Carbon, Nitrogen, and Oxygen

The C, N, and O are not products of a differential analysis of an M giant with respect to the K giant α Tau. One check for systematic errors is then to compare the C, N, and O abundances for α Tau with published results for other G and K giants. For α Tau, we obtain [^{12}C/Fe] = -0.29, [^{14}N/Fe] = $+0.36$, and [^{16}O/Fe] = -0.15 (see Table 10). Using a different mix of atomic and molecular lines, Lambert and Ries (1981) obtained the following mean values for 26 G and K giants: [C/Fe] = -0.24, [N/Fe] = $+0.38$, and [O/Fe] = $+0.01$. Certainly, the C and N abundances for α Tau are in excellent agreement with expectation. The slight O deficiency is probably not significant in light of the sensitivity of the O abundance to effective temperature (Table 4). We do not confirm Lambert and Ries' claim that α Tau stands apart from other G and K giants in having an unusually high C/N ratio. Their result, peculiar to α Tau, must reflect an error somewhere in their analysis of this star.

In our discussion of the M and MS giants, we examine first the M giants and look for evidence of CN-processed material dredge-up by the giant's convective envelope. We consider the ratio [X/Fe]. A normalization to the iron abundance reduces the scatter introduced by differing initial (main-sequence) compositions. We assume that the giant's Fe abundance specifies uniquely the initial C, N, and O abundances according to the recipe [C/Fe] = [N/Fe] = 0 and [O/Fe] = 0.5 [Fe/H] (Clegg, Lambert, and Tomkin 1981). The six M giants give [C/Fe] = -0.14 ± 0.09, [N/Fe] = $+0.44 \pm 0.13$, and [O/Fe] = -0.08 ± 0.08; histograms constructed from our results are shown in Figure 5. This is clear evidence that CN-cycled material contaminates the atmospheres. A signature of CN-cycling is the conservation of the total number of C and N nuclei: we find [(C + N)/Fe] = $+0.03 \pm 0.07$, i.e., C and N nuclei were conserved as CN-cycled material lowered the C abundance and raised the N abundance. The dredge-up by the convective envelope is predicted to leave the O abundance unchanged. Our analyses are fully consistent with this prediction. The dredge-up must also increase the ^{13}C content. Clearly, this has

TABLE 10
C, N, AND O ABUNDANCES

	[Fe/H][a]	[^{12}C/Fe]	[^{14}N/Fe]	[^{16}O/Fe]	[(C + N + O)/Fe]	^{12}C/^{16}O	^{12}C/^{14}N
α Tau	0.00	-0.29	$+0.36$	-0.15	-0.12	0.41	1.07
β Peg	-0.12	-0.10	$+0.39$	$+0.02$	$+0.03$	0.43	1.55
β And	-0.10	-0.04	$+0.48$	$+0.02$	$+0.06$	0.49	1.78
σ Vir	$+0.08$	-0.22	$+0.21$	-0.22	-0.17	0.56	1.78
ν Vir	-0.06	-0.09	$+0.40$	$+0.07$	$+0.05$	0.41	1.74
HR 5299	-0.10	-0.11	$+0.51$	-0.11	-0.02	0.56	1.15
o^1 Ori	-0.03	-0.09	$+0.53$	-0.09	0.00	0.56	1.15
HR 363	-0.12	$+0.20$	$+0.40$	$+0.19$	$+0.21$	0.58	3.02
30 Her	-0.06	-0.29	$+0.62$	-0.10	-0.03	0.36	0.59
HR 6702	0.00	-0.15	$+0.61$	-0.14	-0.02	0.55	0.83

[a] This is the average of the Fe and Ni abundances.
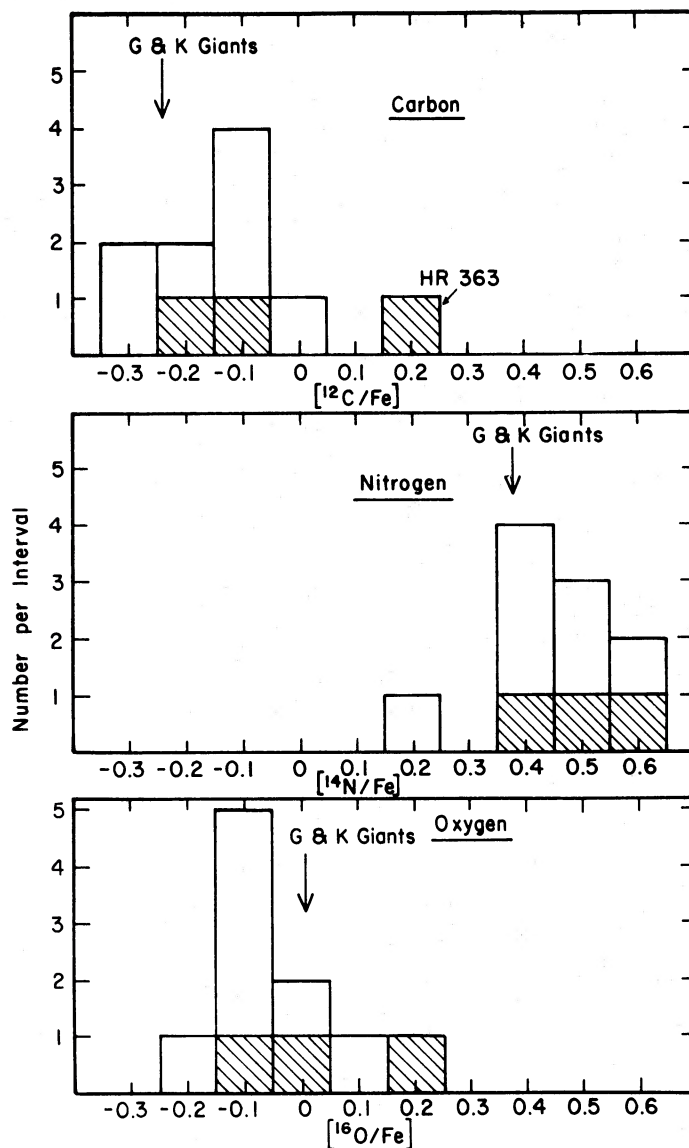
FIG. 5.—The frequency distribution for the CNO abundances in the 10 red giants in this study. The 3 MS giants are indicated by the cross-hatched squares.

happened; the $^{12}C/^{13}C$ ratio for the M giants runs from $^{12}C/^{13}C = 8$ (β Peg) to $^{12}C/^{13}C = 13$ (δ Vir) when the initial value was surely in the range $^{12}C/^{13}C \approx 60$–89. These changes in the ^{12}C, ^{13}C, and ^{14}N abundances and the lack of a change in the ^{16}O abundance are pleasingly similar to earlier results for G and K giants which Lambert and Ries showed to be in qualitative agreement with the predictions. However, standard stellar evolutionary sequences (Dearborn, Tinsley, and Schramm 1978; Shadick, Falk, and Mitalas 1980) cannot account quantitatively for the changes induced by the dredge-up. In particular, the observed $^{12}C/^{13}C$ ratios are far lower than the predicted ratios, which run from $^{12}C/^{13}C \approx 26$ for a 1 $M_\odot$ star to $^{12}C/^{13}C \approx 21$ for $M \gtrsim 2$ $M_\odot$. Some G and K giants also show a low (<15) $^{12}C/^{13}C$ ratio. Lambert and Ries (1981) speculated that the low $^{12}C/^{13}C$ ratios were a consequence of a slow, extensive mixing within the main-sequence star which resulted in the production of copious amounts of ^{13}C but little ^{14}N. If our sample proves to be representative, this slow mixing was common in the progenitors of normal M giants.

Of the three MS stars, HR 363 is the most heavily enriched in the heavy elements (see below) and, also, in ^{12}C (Table 10). This correlation is consistent with the expectation that, at the site for the s-process, the burning must occur before or during the release of the neutrons. We note, however, that HR 363 also shows the largest ^{16}O abundance in the sample. Whether this reflects some error in the analysis of HR 363 or the possibility that new ^{12}C (α, γ) ^{16}O rates (Caughlan et al. 1984) will allow more ^{16}O production in the He-burning shell remains to be seen. Clearly, more cool giants with heavy-element excesses need to be studied. We show in the next section that the lack of a detectable C enrichment in the other two MS stars may not be surprising.

d) The Heavy Elements

If the three MS stars are excluded, the M giants, with one possible exception, show normal abundances of the heavy elements: Sr, Y, Zr, Ba, and Nd. The sole exception may be 30 Her, the coolest star in our sample. Zirconium is the best represented of the heavy elements, and its mean abundance in the
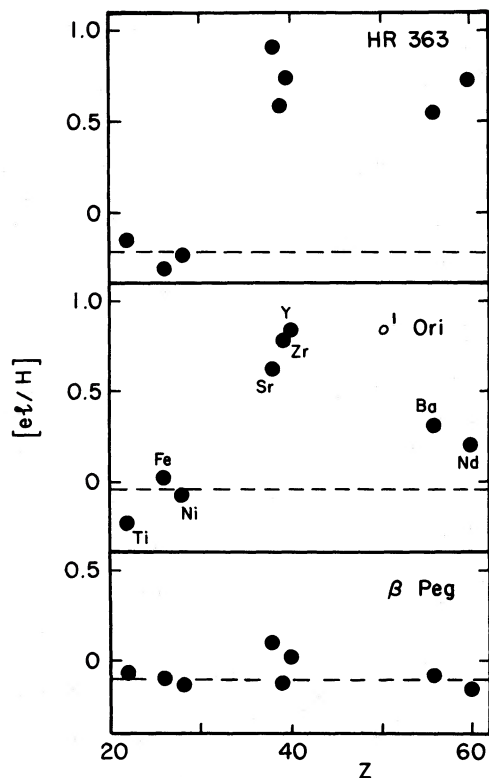
FIG. 6.—Abundances of the heavy elements in three red giants. The dashed lines illustrate the approximate values of [Fe/H]. β Peg shows normal heavy-element abundances, while both HR 363 and o^1 Ori (both MS stars) show enhancements of the heavy elements. Note that the abundance of Ba and Nd is significantly larger relative to Sr, Y, and Zr in HR 363 than in o^1 Ori. These abundances are relative to the comparison star α Tau.

because the abundance analysis of this cool star may be affected adversely by a blanket of TiO lines.

A least-squares fit of the s-process abundance pattern for HR 363 and o^1 Ori was made to the abundance predictions of Cowley and Downs (1980) for various neutron exposures. Assuming an exponential distribution of neutron exposures, HR 363 is fitted best by $\tau_0 = 0.35 \pm 0.05$, while o^1 Ori is characterized by $\tau_0 = 0.2 \pm 0.07$. The uncertainties in these exposures are based upon the recipe of Lampton, Margon, and Bowyer (1976) for fitting data to a one-parameter model (in our case, the integrated neutron exposure) and represent the limits for a confidence of fit greater than 90%.

HR 363, with the largest s-process enhancement and integrated neutron exposure, is also the most ^{12}C-rich. It is surely significant that the C and s-process enhancements are both comparable to the levels reached in the classical barium giants of spectral types G and K. This correspondence is shown clearly by Figure 7; [s/Fe] is a mean of the [Y/Fe] and [Nd/Fe] values. This diagram is similar to that found in Lambert (1984) except for the addition of the M and MS giants. Points for the G and K giants are from Lambert and Ries (1981), the mild Ba stars from Sneden, Lambert, and Pilachowski (1981), and classical Ba stars from Kovács (1983b), Tomkin and Lambert (1983), and Smith (1984). The solid line shows how the composition of a G or K giant would change if increasing amounts of s-process and carbon-rich material, as seen in the "cool" carbon stars (Eriksson et al. 1984), were mixed into the atmosphere.

The relative rates of C and s-process production within a star are not an intrinsic and invariant property of a nuclear-reaction network but rather reflect the detailed structure of particular zones within the interior. In short, mixing resulting from the He core flash in a low-mass star and mixing from thermal pulses in an AGB star are unlikely to produce similar

five M stars (30 Her being excluded) is [Zr/H] = +0.10 and [Zr/Fe] = +0.15. If unweighted means s over the five heavy elements are formed, the grand means for the 5 M stars are [s/H] = +0.05 and [s/Fe] = +0.13. Then, there is a hint in the [s/Fe] values that the M giants may be enriched very slightly in the heavy elements. However, a detailed non–LTE analysis is necessary to show that the enrichment is not a reflection of incompletely canceled departures from LTE. This contrasts with the recent results of Orlov and Shavrina (1984), who find that Mo and Ru are 20 times less abundant relative to H in β Peg than in the Sun. However, their results are based on the laboratory gf-values of Corliss and Bozman (1962) and on lines in the region near 4000 Å where continuum placement is difficult.

The three MS stars and 30 Her appear to fall into two groups. In the first group, characterized by significantly greater enrichments for Sr, Y, and Zr than for Ba and Nd, we find o^1 Ori, HR 6702, and 30 Her. HR 363 stands alone in the second group, for which similar enrichments are found for all five heavy elements. Figure 6 illustrates the differences between the two groups. The abundance pattern for HR 363 is remarkably similar to that displayed by the classical barium giants of spectral types G and K. Bond (see brief comments by McClure 1984) has identified a set of barium and CH stars in which the line enhancements are slight for Ba and the rare earths but strong for Sr, Y, and Zr. He calls these "marginal" barium or CH stars; o^1 Ori, HR 6702 and 30 Her are "marginal" MS stars. Our assignment of 30 Her to the group is tentative

FIG. 7.—The abundance of s-process elements and carbon in barium stars, G and K giants, and the M and MS stars. The solid line shows how the composition of a G or K giant would change with the addition of increasing amounts of material representative of the composition of a cool carbon star. The fraction of added material is indicated along the line.

enhancements for C or s-process elements. The close correspondence between the classical barium and the MS stars suggests that their C and s-process enhancements come from sites with similar characteristics. This is an important clue to the origin of these two classes of peculiar stars.

e) The Evolutionary Status of the MS Stars

Thermal pulses experienced by AGB stars may, through the addition of carbon, convert the O-rich atmosphere of an M giant into the C-rich atmosphere of a cool carbon star. A majority of MS stars are presumably AGB stars which have experienced a few thermal pulses, and the small C enrichment has left oxygen as more abundant than carbon in the atmosphere. A thorough analysis of a large sample of M, MS, and S stars will provide essential data on the initial phases of the thermal pulsing or third dredge-up phase.

The four s-process enriched stars (three MSs and 30 Her) are the four most luminous stars in our sample. Until recently, theoretical calculations predicted that the dredge-up of C and s-process elements would occur only in intermediate-mass stars with relatively large core masses ($M_c \gtrsim 0.8 \ M_\odot$ or $M \gtrsim 6 \ M_\odot$) and at high (quiescent) luminosities (log $L/L_\odot \gtrsim 4.3$)—see, for example, Iben (1984), Iben and Renzini (1983), Wood (1981). Although low-mass stars with reduced core mass begin thermal pulses at lower luminosities (for example, a Population I 2 $M_\odot$ star experiences its first pulse at log $L/L_\odot \sim 3.4$ [Wood 1981]), models failed to predict a dredge-up. Recently, Iben and Renzini (1982) have claimed that when the opacity of the carbon-rich zones is computed more accurately, a dredge-up also occurs in these low-mass stars. Iben (1983) followed thermal pulses of a 1 $M_\odot$ Population I star, and the surface C/O ratio increased from 0.55 to 0.81 by log $L/L_\odot = 3.57$. This luminosity would allow the three MS stars to be identified as low-mass AGB stars, and perhaps 30 Her (log $L/L_\odot \approx 4.0$) as being an intermediate-mass star in the initial phases of third dredge-up. However, the calculations for the low-mass Population I composition do not provide an adequate neutron source. We suppose that, after the theoretical

predictions are further refined, it will be shown that protons can be mixed with the C-rich zones to ignite the ^{13}C neutron source, i.e., ^{12}C (p, γ) ^{13}N $(\beta+, \nu)$ ^{13}C (α, n) ^{16}O.

Earlier we remarked that the similar levels of C and s-process enrichment suggested a link between the MS and the barium stars. Mass transfer across a binary is that link. Those MS stars which are in binary systems in which mass transfer by Roche-lobe overflow occurs as the MS star evolves up the AGB will convert their companions to barium stars.

V. CONCLUDING REMARKS

The principal novel result of this study is the demonstration that thorough abundance analyses providing key clues to the nucleosynthesis and mixing experienced by M giants are possible through a selection of windows in the near-infrared and infrared. Thoroughly plausible results for normal M giants provide the confidence to interpret the results for MS giants in terms of the predicted dredge-up phases for red giants.

Before the dredge-up phases are understood fully, a much larger sample of red giants must be analyzed. Many questions call for answers. Can one find stars which have undergone dredge-up after only one or two pulses? Do intermediate-mass stars dredge up s-process elements synthesized with ^{22}Ne (α, n) ^{25}Mg as the neutron source (a speculation: are marginal MS stars such as o^1 Ori, HR 6702, or 30 Her intermediate-mass stars?)? An inherent property of the ^{22}Ne source is that it produces rather small amounts of Ba and the rare earths. In low-mass stars where ^{13}C (α, n) ^{16}O is the presumed neutron source, does the average neutron exposure vary from pulse to pulse?

REFERENCES

Anders, E., and Ebihara, M. 1982, Geochim. et Cosmochim., 46, 2363.
Becker, S. A. 1981, Ap. J. Suppl., 45, 475.
Becker, S. A., and Iben, I., Jr. 1979, Ap. J., 23, 831.
———. 1980, Ap. J., 237, 111.
Beer, R. 1974, private communication.
Bell, R. A., Edvardsson, B., and Gustafsson, B. 1984, M.N.R.A.S., in press.
Bessell, M. S., and Wood, P. R. 1984, Pub. A.S.P., 96, 247.
Boesgaard, A. M. 1970, Ap. J., 161, 163.
Brown, J. A., Tomkin, J., and Lambert, D. L. 1983, Ap. J. (Letters), 265, L93.
Caughlan, G. R., Fowler, W. A., Harris, M. J., and Zimmerman, B. A. 1984, Atomic Data Nucl. Data Tables, submitted.
Chackerian, C., Jr., and Tipping, R. H. 1983, J. Molec. Spectrosc., 99, 431.
Clegg, R. E. S., Lambert, D. L., and Tomkin, J. 1981, Ap. J., 250, 262.
Cochran, A. L. 1978, M.S. thesis, University of Texas.
Corliss, C. H., and Bozman, W. R. 1962, NBS Monog., No. 53.
Cowley, C. R., and Downs, P. L. 1980, Ap. J., 236, 648.
Dearborn, D., Tinsley, B. M., and Schramm, D. N. 1978, Ap. J., 223, 557.
Delbouille, L., Neven, L., and Roland, G. 1973, Photometric Atlas of the Solar Spectrum from λ3000 to λ10000 (Liège: Institut d'Astrophysique).
Dominy, J. F., Hinkle, K. H., and Lambert, D. L. 1984, in preparation.
Eggen, O. J. 1972, Ap. J., 177, 489.
Eriksson, K., Gustafsson, B., Hinkle, K. H., and Lambert, D. L. 1984, in preparation.
Grevesse, N., Sauval, A. J., and van Dishoeck, E. F. 1985, Astr. Ap., in press.
Hall, D. N. B., Ridgway, S. T., Bell, R., and Yarborough, J. M. 1978, Proc. Soc. Photo-Optical Instrumentation Engineers, 172, 121.
Hinkle, K. H., and Lambert, D. L. 1975, M.N.R.A.S., 170, 447.
Holweger, H., and Müller, E. A. 1974, Solar Phys., 39, 19.
Huggins, P. J. 1973, Astr. Ap., 28, 217.
Iben, I., Jr. 1983, Ap. J. (Letters), 275, L65.

Iben, I., Jr. 1984, in IAU Symp. 105, Observational Tests of the Stellar Evolution Theory, ed. A. Maeder and A. Renzini (Dordrecht: Reidel), p. 3.
Iben, I., Jr., and Renzini, A. 1982, Ap. J. (Letters), 259, L79.
———. 1983, Ann. Rev. Astr. Ap., 21, 271.
Jaschek, C., Conde, H., and de Sierra, A. C. 1964, Catalogue of Stellar Spectra Classified in the Morgan-Keenan System (La Plata).
Johnson, H. L., Mitchell, R. I., Iriarte, B., and Wiśniewski, W. Z. 1966, Comm. Lunar and Planet. Lab., 4, 99.
Johnson, H. R., Bernat, A. P., and Krupp, B. M. 1980, Ap. J. Suppl., 42, 501.
Kjaergaard, P., Gustafsson, B., Walker, G. A. H., and Hultqvist, L. 1982, Astr. Ap., 115, 145.
Kovács, N. 1983a, Astr. Ap., 120, 21.
———. 1983b, Astr. Ap., 124, 63.
Kurucz, R. L., and Peytremann, E. 1975, Smithsonian Ap. Obs. Spec. Rept., No. 362.
Lambert, D. L. 1981, in Physical Processes in Red Giants, ed. I. Iben, Jr. and A. Renzini (Dordrecht: Reidel), 115.
———. 1984, in Cool Stars with Excesses of Heavy Elements, ed. C. Jaschek and M. Jaschek (Dordrecht: Reidel), in press.
Lambert, D. L., Brown, J. A., Hinkle, K. H., and Johnson, H. R. 1984, Ap. J., 284, 223.
Lambert, D. L., and Ries, L. M. 1981, Ap. J., 248, 228.
Lampton, M., Margon, B., and Bowyer, S. 1976, Ap. J., 208, 177.
Larsson, M., Siegbahn, P. E. M., and Ågren, H. 1983, Ap. J., 272, 369.
Mäckle, R., Holweger, H., Griffin, R., and Griffin, R. 1975, Astr. Ap., 38, 239.
Maillard, J. P., Chauville, J., and Mantz, A. W. 1976, Molecular Spectroscopy, 63, 120.
McClure, R. D. 1984, Pub. A.S.P., 96, 117.
Nishi, N., Shinohara, H., and Hanazaki, I. 1982, J. Chem. Phys., 77, 246.
Orlov, M. Ya., and Shavrina, A. V. 1984, Soviet Astr. Letters, Vol. 10, No 1, 53.

Paczyński, B. 1970, *Acta. Astr.*, **20**, 47.
Pedley, J. B., and Marshall, R. M. 1983, *J. Phys. Chem. Ref. Data*, **12**, 967.
Peery, B. F., Jr. 1971, *Ap. J. (Letters)*, **163**, L1.
Ridgway, S. T., Joyce, R. R., White, N. M., and Wing, R. F. 1980, *Ap. J.*, **235**, 126.
Ruland, F., Holweger, R., Griffin, R., Griffin, R., and Biehl, D. 1980, *Astr. Ap.*, **92**, 70.
Sauval, A. J., Grevesse, N., Brault, J. W., Stokes, G. M., and Zander, R. 1984, *Ap. J.*, **282**, 330.
Scalo, J. M., Dominy, J. F., and Pumphrey, W. A. 1978, *Ap. J.*, **221**, 616.
Shadick, S. J., Falk, H. J., and Mitalas, R. 1980, *M.N.R.A.S.*, **192**, 493.
Smith, V. V. 1984, *Astr. Ap.*, **132**, 326.
Sneden, C. 1974, Ph.D. thesis, University of Texas.
Sneden, C., Lambert, D. L., and Pilachowski, C. A. 1981, *Ap. J.*, **247**, 1052.
Sweigart, A. V., and Gross, P. G. 1978, *Ap. J. Suppl.*, **36**, 405.
Taherian, M. R., and Slanger, T. G. 1984, *J. Chem. Phys.*, in press.

Thompson, R. I. 1973, *Ap. J.*, **181**, 1039.
Tinsley, B. M. 1980, *Fund. Cosmic Phys.*, **5**, 287.
Tomkin, J., and Lambert, D. L. 1983, *Ap. J.*, **273**, 722.
Tsuji, T. 1973, *Astr. Ap.*, **23**, 411.
———. 1981, *Astr. Ap.*, **99**, 48.
———. 1984, in *Cool Stars with Excesses of Heavy Elements*, ed. C. Jaschek and M. Jaschek (Dordrecht: Reidel), in press.
van Dishoeck, E. R. 1984, private communication.
Vogt, S. S., Tull, R. G., and Kelton, P. K. 1978, *Appl. Optics*, **17**, 574.
Werner, J. H., Rosmus, P., and Reinsch, E. A. 1983, *J. Chem. Phys.*, **79**, 905.
Wilson, O. C. 1976, *Ap. J.*, **205**, 823.
Wood, P. R. 1981, in *Physical Processes in Red Giants*, ed. I. Iben, Jr. and A. Renzini (Dordrecht: Reidel), p. 135.
Yamashita, Y. 1965, *Pub. Astr. Soc. Japan*, **17**, 27.
———. 1967, *Pub. Dom. Ap. Obs. Victoria*, **13**, 47.
Yamashita, Y., and Utsumi, K. 1962, *Pub. Astr. Soc. Japan*, **14**, 208.

DAVID L. LAMBERT and VERNE V. SMITH: Department of Astronomy, University of Texas, Austin, TX   78712